

Article

Architectural Framework and Feasibility of Internet of Things-Driven Mars Exploration via Satellite Constellations

Oscar Ledesma ^{1,*} , Paula Lamo ^{1,*} , Juan A. Fraire ^{2,3}, María Ruiz ⁴ and Miguel A. Sánchez ¹ 

¹ Escuela Superior de Ingeniería y Tecnología, Universidad Internacional de La Rioja, 26006 Logroño, Spain; miguelangel.sanchez@unir.net

² Inria, INSA Lyon, CITI, UR3720, 69621 Villeurbanne, France; juan.fraire@inria.fr

³ CONICET, Universidad Nacional de Córdoba, Córdoba 5000, Argentina

⁴ Centro de Astrobiología (CAB), INTA-CSIC, 28850 Madrid, Spain; mruiz@cab.inta-csic.es

* Correspondence: oscar.ledesma.garcia@unir.net (O.L.); paula.lamo@unir.net (P.L.)

Abstract: This study outlines a technical framework for Internet of Things (IoT) communications on Mars, leveraging Long Range (LoRa) technology to connect Martian surface sensors and orbiting satellites. The designed architecture adapts terrestrial satellite constellation models to Martian environments and the specific needs of interplanetary communication with Earth. It incorporates multiple layers, including Martian IoT nodes, satellite linkage, constellation configuration, and Earth communication, emphasizing potential Martian IoT applications. The analysis covers four critical feasibility aspects: the maximum communication range between surface IoT nodes and orbiting satellites, the satellite constellation's message processing capacity to determine IoT node volume support, the communication frequency and visibility of IoT nodes based on the satellite constellation arrangement, and the interplanetary data transmission capabilities of LoRa-based IoT devices. The findings affirm LoRa's suitability for Martian IoT communication, demonstrating extensive coverage, sufficient satellite processing capacity for anticipated IoT node volumes, and effective data transmission in challenging interplanetary conditions. This establishes the framework's viability for advancing Mars exploration and IoT in space exploration contexts.



Citation: Ledesma, O.; Lamo, P.; Fraire, J.A.; Ruiz, M.; Sánchez, M.A. Architectural Framework and Feasibility of Internet of Things-Driven Mars Exploration via Satellite Constellations. *Electronics* **2024**, *13*, 1289. <https://doi.org/10.3390/electronics13071289>

Academic Editors: Federica Rinaldi, Chiara Suraci and Helka-Liina Määttänen

Received: 28 February 2024

Revised: 25 March 2024

Accepted: 28 March 2024

Published: 30 March 2024



Copyright: © 2024 by the authors. Licensee MDPI, Basel, Switzerland. This article is an open access article distributed under the terms and conditions of the Creative Commons Attribution (CC BY) license (<https://creativecommons.org/licenses/by/4.0/>).

Keywords: IoT; LoRa; Mars; satellite; NewSpace; framework; feasibility study

1. Introduction

The potential of the Internet of Things (IoT) in space exploration has been demonstrated [1] through technological advancements in satellite communications, cloud computing, artificial intelligence, and machine learning. A new extension of IoT, the Internet of Space Things (IoST), has been developed. It utilizes small satellites like nanosatellites [2] in low Earth orbit (LEO) to offer global coverage in space [3,4], along with significantly more flexible network access services [4]. These satellites are low-cost and have a simplified design, which has allowed for the development of new applications and services in space, such as earth observation and technological demonstrations, with the most widespread applications being related to the telecommunications domain [5].

As the interest in deep space exploration grows, planning large-scale space missions and formulating space architecture has become essential. Both public space agencies and private companies [6] have announced plans for Mars exploration in the coming years. Initially, missions were based on communication systems limited in bandwidth and transmission time [7]. However, in recent decades, new technologies have been implemented, such as autonomous rovers equipped with cameras and sensors for atmospheric and geological research [8], including drones, to improve and expand exploration areas [9]. In this context, small satellite constellations are already beginning to be used [10], significantly extending the coverage and simplifying the acquisition of measurements in various locations on the planet. This could enable the deployment of constellations in planetary

orbit, facilitating IoT communications with sensors on the surface [11], similar to how the deployment is handled on Earth.

In this context, recent research lines on the massive deployment of IoT devices, as illustrated in [12], may apply to Martian exploration through the extensive deployment of IoT devices on the Martian surface. Authors in [12] discussed the enhancement of the efficiency in massive IoT systems using reconfigurable intelligent surfaces (RISs). This study proposes the integration of mixed analog-digital converters (ADCs) to optimize system performance and hardware load, accompanied by a nonlinear theoretical analysis that addresses channel estimation and activity detection based on Bayesian theory for massive deployments. Furthermore, research on sixth generation (6G) networks, as presented in [13], should be considered for future networks, providing a comprehensive overview of channel modelling and feature analysis.

In the exploration of Mars with IoT, various architectures that can be deployed are presented, each with their limitations and considerations, as in [14]. These architectures can vary in terms of the communication technology used, the arrangement of IoT nodes and satellites, and the integration with interplanetary communications systems. It is essential to develop reliable and efficient communications, considering options such as using low-power wide area network (LPWAN) technologies and optimizing coverage and data processing capacity. Good architectural design is essential to ensure the viability of deployments in complex planetary environments such as Mars [15]. Significant aspects to consider include the transmission distance, the message processing capacity of the satellites, the communication frequency, the configuration of the satellite constellation, the revisit and visibility times of the IoT nodes with the satellites, and interplanetary communications between Mars and Earth. However, studying these architectures and communications is still challenging and requires implementing specific architectures for future Mars exploration [15].

In this context, the study aims to establish a reference architecture for using satellite constellations in Mars orbit and evaluate the feasibility of IoT communications. It aims to define the communication architecture of IoT, analyze the optimal satellite constellation, develop a model of interplanetary communications between Mars and Earth, evaluate Long Range (LoRa) communications on Mars, and identify potential IoT applications on the red planet. To achieve this, various technical and analytical activities will be carried out. This will include the design of communications infrastructure, encompassing IoT nodes, satellites, and interplanetary communication systems. The spatial layout and number of satellites necessary to guarantee adequate coverage on the Martian surface will also be determined. Data transmission systems will be analyzed to overcome the distances and unique conditions of the interplanetary environment for communications between Mars and Earth. Likewise, the feasibility and effectiveness of LoRa communications on Mars will be evaluated, considering factors such as transmission distance and message processing capacity. Specific scenarios, such as atmospheric, geological, and seismic monitoring, will be explored to maximize IoT's potential in exploring the red planet. These activities are essential for developing a suitable communications infrastructure and successfully implementing the IoT in the Martian context.

This manuscript starts with Section 2, which is dedicated to examining the architecture suggested for its implementation in detail. Subsequently, Section 3 addresses the study of communication between IoT nodes and satellites in Martian orbit, considering aspects such as transmission distance, message capacity, the design of the satellite constellation, and the frequency of communications through LoRa and interplanetary data communications. This section lays the foundation for Section 4, which presents the results obtained from the simulations. Section 5 details the potential applications of IoT in this context, while Section 6 explains the open research challenges and future directions. The document concludes with the presentation of the conclusions.

2. Proposed Architecture for Mars Exploration with IoT

To implement an IoT solution on the surface of Mars using satellite constellations, it is necessary to reconfigure and adapt the architecture currently used in terrestrial satellite constellations [14,16]. Also, the new architecture must be integrated with the pre-existing communications systems between both planets [11].

As shown in Figure 1, the satellite IoT solution on Earth comprises five fundamental layers [14,17]. In the first layer, there are IoT nodes, whose function is to acquire data from the physical environment and send it through low-power area network (LPWAN) communications to satellites in LEO. These satellites make up the next layer, consolidate data transmissions, and forward the data received from the IoT nodes to the ground station. In the third layer, the ground station receives the satellite data. It forwards it to the core layer or network server, which monitors and regulates the communications between the IoT nodes and the satellites and performs data ingestion. The network core, or network server, is responsible for transmitting data from IoT nodes to business applications and carries out authentication, authorization, and accounting tasks to ensure adequate security of services. Finally, the last layer is the application layer, which receives data from the satellite network for processing and displays it to the user.

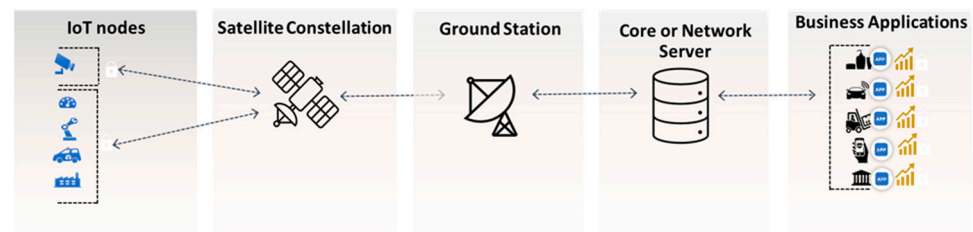


Figure 1. Satellite IoT terrestrial architecture.

In the scenario involving Mars, it is crucial to integrate the IoT satellite communications architecture with the interplanetary communications system. Earth and Mars communicate through orbiters, which act as intermediaries for communication between missions on the Martian surface and ground stations. This helps to improve contact opportunities and direct communication time with Earth [18]. Orbiters in Mars orbit can carry high-gain X-band antennas that provide high-speed communications with Earth [19]. The constellation of satellites can use the orbiter as a relay to transmit data collected by IoT nodes to Earth. Communications between the satellites of this constellation would be carried out through Inter-Satellite Links (ISLs) using S-band frequencies [20]. Consequently, it is essential to characterize the communication dynamics between Earth and Mars to ensure the success of interplanetary communications and, therefore, the adequate support of Martian missions that use IoT technology. This involves considering the relationship between distance, transmission time, and frequency of contacts, considering orbital mechanics and the location of ground stations on Earth.

Considering the above, the proposed interplanetary exploration IoT architecture consists of six fundamental layers, as shown in Figure 2:

- **IoT nodes**: Refers to the devices and sensors deployed on Mars to analyze atmospheric aspects (e.g., temperature, pressure, gas measurement, and air quality) and geological aspects (e.g., seismic movements). These nodes share characteristics with terrestrial IoT nodes with LPWAN satellite communications, such as long battery life, low cost, and miniaturization. However, they must have enhanced protection against space radiation on Mars compared to Earth [21], as well as the problems associated with dust storms [22], extreme temperature [23], and high space radiation due to the lack of a magnetic field [24] and its tenuous atmosphere [25]. In that sense, the National Aeronautics and Space Administration (NASA) is making significant efforts to adopt IoT for space applications [11].

- **Satellite constellation:** The concept refers to satellites designed to meet a common objective, centrally coordinated, and deployed in orbit [26]. Unlike individual satellites, a constellation ensures the simultaneous presence of multiple satellites in different areas of Mars, allowing for extended coverage. These satellites are organized into orbital planes with similar altitudes and angles, which operate as an interconnected network to provide global coverage across the planet [27].
- **Orbiter satellite:** The orbiter satellite acts as a communication link between the Martian surface and the Earth and is located 300 km above the Martian surface [28,29]. Given the distance between Mars and Earth, the direct signal that equipment such as rovers can send is weak, so the orbiters act as signal amplifiers to retransmit them with greater intensity to Earth. They use X-band frequencies to provide a stable and reliable connection with Earth [30].
- **Ground station:** This refers to the antenna located on Earth to receive communications sent by the Martian orbiter. This station is part of the existing infrastructure for communications with Mars orbiters [30] and acts as a bridge with the terrestrial communications infrastructure. The information from the IoT nodes received by the ground station is forwarded to the core or network server.
- **Core or network server:** The network server is in charge of processing, storing, and forwarding satellite data to external applications [17], such as data visualization tools. In the case of LPWAN communications, it manages the authentication, validation, and provisioning of IoT nodes in the network. The processed data are then sent via an application programming interface (API) to applications used by scientists.
- **Scientific applications:** These are applications used by scientists or companies to analyze and study data collected by IoT nodes or other instruments on Mars, such as Java Mission-planning for Analysis and Remote Sensing (JMARS) for atmospheric data analysis [31]. Section 5 of this work details the main applications that can be developed on Mars with this technology, considering the lines of research currently underway or planned to be carried out in the future.

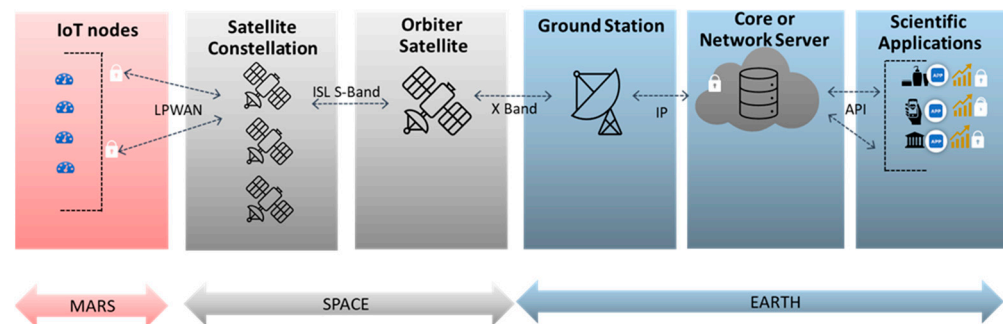


Figure 2. Interplanetary exploration IoT architecture.

IoT nodes and systems must be designed and tested meticulously to ensure their reliability and performance even under extreme conditions. They use materials and components that resist radiation and the vacuum of space [22]. To prevent operational problems, internal thermal control and specific protection systems are implemented [11,23]. Error mitigation techniques are also implemented to ensure the integrity of transmitted data. For terrestrial IoT nodes, hardware-level adaptation can be conducted through dust protection systems, internal thermal control, and protection against space radiation. NASA is currently conducting studies in this area [11]. The feasibility of using electronic devices based on Commercial Off-the-Shelf (COTS) has become a central issue in space mission planning [32]. It has proven to be a transformative strategy to reduce costs and accelerate development timelines. An example of this is the Ingenuity helicopter, which operates on the surface of Mars. It has two cameras and a telecommunications module that depends on COTS components. The Mars Science Laboratory mission also included these components

in the propulsion and parachute systems to guarantee a precise and safe landing [33]. These components are increasingly used in deep space exploration missions [34]. They benefit from advances in miniaturization, energy efficiency, and signal processing. This allows for the construction of smaller, lighter satellites and probes with increasingly greater capabilities and operational autonomy.

As shown in Figure 3, communications between IoT nodes and the satellite constellation in Mars orbit can have two communication models: Direct-to-Satellite IoT (DtS-IoT) and Indirect-to-Satellite IoT (ItS-IoT) [35]. In DtS-IoT communication, IoT nodes communicate directly with the constellation without an intermediary. On the other hand, ItS-IoT needs a gateway that centralizes all communications from nearby IoT nodes. This gateway collects data from IoT nodes and transmits it to the orbiting satellite constellation. Current rovers can be proposed as LoRa gateways for exploration on Mars since they currently act as gateways between sensors and drones with the Earth, such as the Ingenuity helicopter [36]. In the case of gateways, LoRa can be used on rovers or probes on the surface of Mars. It can provide coverage in open spaces of up to 15 km [37].

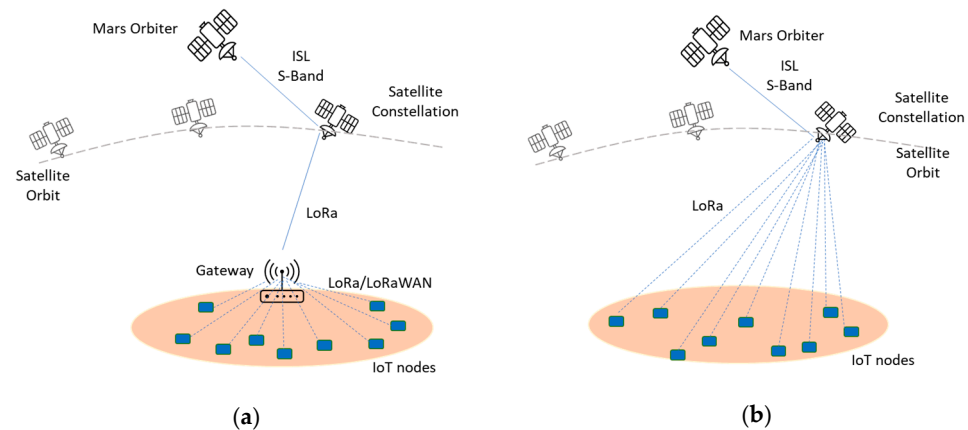


Figure 3. Communication models for nodes: (a) ItS-IoT and (b) DtS-IoT [14].

LPWAN protocols are considered an alternative for the integration of IoT technologies for both terrestrial and space networks [17]. In satellite IoT communications, LoRa/LoRaWAN and Narrowband IoT (NB-IoT) are prominent options for connecting long-range with reduced costs and low energy consumption [38]. Recent research shows the feasibility of establishing direct links with satellites by implementing these protocols [17], enabling direct communication between IoT nodes and satellites in orbit. This can be applied to other planets after redesigning the communication architectures. Between the two options, studies position LoRa/LoRaWAN as an IoT connectivity protocol suitable for exploring Mars or the Moon [11] due to its energy efficiency [14,39,40] and greater robustness against the Doppler effect [14]. Its adaptation to the architecture proposed in Figure 2 focuses on guaranteeing communications between the IoT nodes and the satellites, for which it is necessary to use a LoRaWAN network server (LNS) to manage and administer the communications located physically on Earth. This server collects device data, contextualizes them, and prepares them for application use [14]. Since there is no regulation on the frequencies that can be used on Mars, the use of any terrestrial frequencies used by this technology can be proposed. Therefore, 868 MHz and 433 MHz have been used in this study.

3. Feasibility Analysis of IoT Architecture Utilizing LoRa Communications on Mars

It is proposed that the feasibility of the proposed architecture for exploring Mars using LoRa be evaluated. This will be conducted by analyzing four key aspects in detail: the constellation model and the revisit time of satellites over IoT nodes on the Martian surface, the maximum communication distance between the IoT nodes and the satellites of the constellation, the maximum capacity of messages that each satellite of the constellation can

process to determine the volume of IoT nodes, and the interplanetary data communications of the IoT nodes. Below is a theoretical description of the evaluation process.

3.1. Analysis of the Constellation Model and the Revisit Time of Satellites over IoT Nodes

When planning the deployment of satellite constellations for data collection, it is essential to consider the optimal constellation model and the revisit time of satellites over IoT nodes. In that sense, it is possible to propose two models: Walker Delta and Walker Star. Both are widely used in communication satellite constellations on Earth [41]. The Walker Delta model is characterized by a triangular arrangement of satellites in orbit and greater redundancy in communication. This configuration provides better coverage of areas near the equator. However, it does not adequately cover the poles, providing partial planet coverage [42]. The Walker Star model has an inclination angle close to 90 degrees [41] to provide complete global coverage, including the polar regions [43]. That is why the model that we propose, due to its greater capacity to provide coverage to the polar regions, and the one used in the study, is the Walker Star. Figure 4 shows both models, highlighting the satellites' coverage areas and orbital movements. Given the complexity of exploring the poles of Mars and the need to understand the interrelationship between polar deposits and its climate system, there is significant scientific interest in exploring Mars at high latitudes [16].

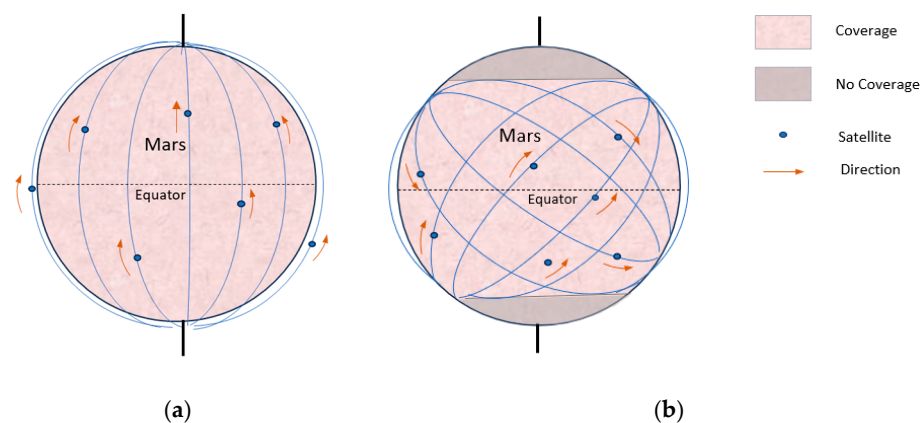


Figure 4. Constellation models: (a) Walker Star and (b) Walker Delta.

Satellite revisit refers to the time interval that elapses between two successive passes of a satellite over an exact location on the planet's surface. This is a critical factor that influences the efficiency and frequency with which satellites in a constellation pass over a specific point on Mars and the visibility time of those satellites by IoT nodes. For its part, the factors that influence the determination of the revisit of a satellite over a specific point on the planet are the arrangement of the constellation, the orbital height, the inclination, and the latitude of the object in question [44]. The variation in revisit times and visibility of satellites over IoT nodes on Mars has significant implications for the planning and operation of space missions on the red planet. A greater revisit time allows for more frequent communication and more efficient data collection, while longer visibility times increase the window of opportunity for data transmission. On the other hand, the greater the inclination angle of the satellite to the equator, the greater the coverage at higher latitudes, as shown in Figure 4, ensuring coverage in the polar regions.

3.2. Analysis of the Transmission Distance between IoT Node and Satellite in Martian Orbit

This analysis aims to assess whether it is possible to establish communication between IoT nodes on the surface of Mars and satellites orbiting the planet. Furthermore, the analysis intends to determine the signal strength emitted by the IoT nodes utilizing LoRa technology. The assessment will include testing the transmission range to determine if the signal power is strong enough to be received by a satellite in a specific orbit.

An important factor for conducting the study is the maximum distance at which IoT nodes can reliably communicate with orbiting satellites. This is calculated using mathematical formulas and models. One of the most widely used methods is the radio propagation model for transmission distance estimation, also known as the Friis equation [45] (see Equation (1)), which establishes a fundamental relationship between free space losses, antenna gains, wavelength, reception, and transmission powers [45].

$$P_{Rx} = P_{Tx} G_{Tx} \left(\frac{\lambda}{4\pi R} \right)^2 G_{Rx} \quad (1)$$

where P_{Rx} is the received power; P_{Tx} is the transmission power; G_{Tx} is the transmitter antenna gain; G_{Rx} is the receiver antenna gain; R is the maximum distance, with a direct line of sight, between the transmitter and the receiver; and λ is the wavelength of the transmission frequency. According to the equation, communication between IoT nodes on Mars's surface and orbiting satellites is possible if the received power is greater than the satellite antenna's sensitivity.

In the model developed, the effect of atmospheric attenuation on Mars has been neglected because the density of the Martian atmosphere is much lower than that of Earth. The atmospheric pressure on Mars is about one hundred times lower [46] than Earth's, and the attenuation caused by water vapor is 3086 times lower. Consequently, it is estimated that said attenuation is negligible for radio communications [30]. Furthermore, it should be noted that a significant portion of the communication between the IoT node and the satellite occurs through space, devoid of gases, obstacles, or intervening elements that could affect signal transmission.

3.3. Analysis of the Maximum Message Capacity of Satellites

This analysis focuses on evaluating the capacity of satellites to receive messages from IoT nodes and, consequently, estimating the number of IoT nodes that could be deployed on the surface of Mars according to the proposed architecture. The communication capacity of each satellite is calculated using LoRa technology, considering the data transmission speed. To conduct this analysis, the theoretical maximum message capacity will be calculated for the satellite's orbital period, determined by Kepler's Third Law [47].

Also, the transmission rate must be considered based on the different spreading factors (SFs). From the SFs, the transmission data rate from the IoT nodes to the satellites in orbit can be determined and, thus, the number of messages each satellite can receive in its orbital period. The LoRa protocol uses various SFs to determine the type of communication, which determines the spectral efficiency of the transmission and affects the data rate [48].

The different available SFs have varying transmission rates that impact the message capacity each satellite can manage during each orbital period. By evaluating these rates, it is possible to determine the theoretical number of messages each satellite can receive and the volume of IoT nodes that can be deployed based on the data rates and package duration associated with each SF [49].

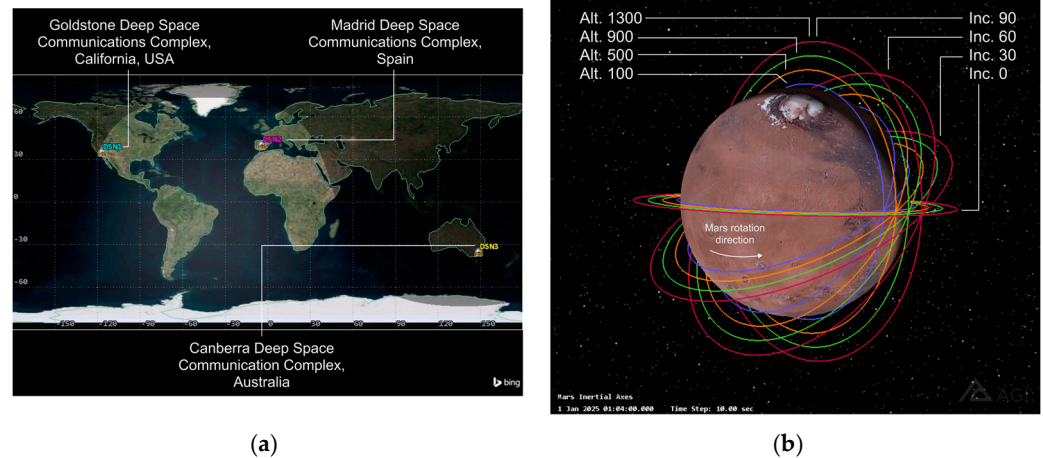
3.4. Analysis of the Interplanetary Communications for the Proposed Architecture

Establishing good communication between Mars and Earth is vital for the proposed architecture's success. Therefore, proposing an analysis of interplanetary communications to address in detail the characteristics of Earth–Mars communications, such as distance, signal propagation time, and contact frequency (number of contacts in a time interval), is essential to guaranteeing the system's efficiency and reliability.

This assessment examines the characteristics of the communication links between Earth, represented by NASA's Deep Space Network (DSN) [31], and a series of hypothetical Mars orbiters. The DSN consists of three ground stations in Goldstone, California, USA; Madrid, Spain; and Canberra, Australia. These stations are strategically positioned around the globe to allow for continuous communication with spacecraft as Earth rotates (see Table 1 and Figure 5).

Table 1. NASA’s DSN ground stations.

| Location | Latitude | Longitude | Altitude (km) |
|---------------------|------------|-------------|---------------|
| Goldstone, CA, USA | 35.4266° N | 116.8899° W | 1.0 |
| Madrid, Spain | 40.4316° N | 4.2491° W | 0.8 |
| Canberra, Australia | 35.4020° S | 148.9819° E | 0.7 |

**Figure 5.** DSN and Mars orbit scenarios. (a) NASA’s Deep Space Network (DSN). (b) Mars orbital scenario and parameters.

To conduct this study, sixteen distinct orbits for the Mars segment have been defined, each characterized by a specific semi-major axis and inclination. The altitudes of these orbits above the Martian surface are set at 100, 500, 900, and 1300 km with inclinations at 0, 30, 60, and 90 degrees. These orbits have been selected to provide a comprehensive overview of potential operational environments for spacecraft around Mars, especially for the ISL with the satellite constellation (see Table 2).

The lower-altitude orbits (100 km) represent low Mars orbit (LMO) missions, enabling high-resolution observation or efficient Martian surface and atmosphere data collection. These are particularly useful for scientific research, such as studying Martian geology or searching for water sources. The medium-altitude orbits (500 and 900 km) can be representative of communication and weather satellites, providing broader coverage and serving as relays for missions on the Martian surface. The high-altitude orbit (1300 km) would represent areostationary or areosynchronous orbits (terms analogous to “geostationary” and “geosynchronous” orbits used for Earth satellites but applied to Mars), which could be advantageous for constant communication coverage over specific areas of the Martian surface and the ISL with the satellite constellation.

The range of inclinations from equatorial (0 degrees) to polar (90 degrees) ensures that the study encompasses different mission profiles. The given scenario’s duration is set from 1 January 2025, for twice the synodic period ($780 \text{ days} \times 2$), totaling approximately 1560 days or about 4.2 years. The synodic period of Earth and Mars is the time required for Earth and Mars to return to the same positions relative to each other and the Sun, allowing for the reoccurrence of similar geometric relationships between the two planets. This period is approximately 780 days or about 2.1 years. This duration is particularly representative for assessing the Earth–Mars communication link because it covers two complete synodic cycles.

Table 2. Studied Mars orbits.

| Semi-Major Axis (km) | Altitude (km) | Eccentricity | Inclination (Degrees) | T. Anom. (Degrees) | RAAN (Degrees) | Arg. of P. (Degrees) |
|----------------------|---------------|--------------|-----------------------|--------------------|----------------|----------------------|
| 3496 | 100 | 0 | 0 | 0 | 0 | 0 |
| 3496 | 100 | 0 | 30 | 0 | 0 | 0 |
| 3496 | 100 | 0 | 60 | 0 | 0 | 0 |
| 3496 | 100 | 0 | 90 | 0 | 0 | 0 |
| 3896 | 500 | 0 | 0 | 0 | 0 | 0 |
| 3896 | 500 | 0 | 30 | 0 | 0 | 0 |
| 3896 | 500 | 0 | 60 | 0 | 0 | 0 |
| 3896 | 500 | 0 | 90 | 0 | 0 | 0 |
| 4296 | 900 | 0 | 0 | 0 | 0 | 0 |
| 4296 | 900 | 0 | 30 | 0 | 0 | 0 |
| 4296 | 900 | 0 | 60 | 0 | 0 | 0 |
| 4296 | 900 | 0 | 90 | 0 | 0 | 0 |
| 4696 | 1300 | 0 | 0 | 0 | 0 | 0 |
| 4696 | 1300 | 0 | 30 | 0 | 0 | 0 |
| 4696 | 1300 | 0 | 60 | 0 | 0 | 0 |
| 4696 | 1300 | 0 | 90 | 0 | 0 | 0 |

where T. Anom. is true anomaly; RAAN, right ascension of the ascending node; and Arg. of P., argument of perigee.

Each DSN station's unique geographical location and altitude offers a different look angle and communication window with each orbiter, making this analysis robust and significant for future Mars IoT mission planning and support. By evaluating these links, we can understand the challenges and capabilities of Earth-to-Mars communication, which is critical for efficient data backhauling between the IoT access network and the core or network server on Earth.

4. Results

This section demonstrates the feasibility of using standard LoRa parameters in satellite constellations in LEO orbits for IoT communications on Mars through a detailed use case simulation (see Table 3). The revisit and visibility times of the IoT nodes are also evaluated according to the configuration of the satellite constellation, the transmission distance, the message processing capacity of the satellites, and the interplanetary data communications between Mars and the Earth.

To calculate revisit times and the visibility of IoT nodes, several commercial applications are used for the satellite dynamics' simulation [50]; among them is the System Tool Kit (STK) software [2], which is used in this work. To complete this study, STK analyzed Martian orbiter trajectories precisely, considering various factors that affect satellite motion. After establishing the required orbital propagations and communication links within STK, the data were exported to comma-separated value (CSV) files for further handling. Various key metrics were examined during the post-processing phase of the data analysis. One of these metrics is the visibility time of satellites. It measures the duration between the initiation and termination of contact between a satellite from the constellation and an IoT node located on the surface of Mars. Another metric is the revisit time, which refers to the duration required for a Mars orbiter to pass over a specific IoT node on Mars again. These metrics are crucial for assessing the viability and reliability of communications between the satellite constellation and IoT nodes on the Mars surface and are discussed below. The code for creating the STK scenario, exporting the data, and processing and plotting the results can be seen in the repository of the Data Availability Statement.

Table 3. Satellite revisit times based on constellation size at 90-degree inclination about orbit altitude and IoT node latitude.

| Constellation No. | No. Satellites | Orbital Planes | IoT Node Latitude (Degrees) | Revisit Time (Minutes) 100 km Altitude | Revisit Time (Minutes) 500 km Altitude | Revisit Time (Minutes) 900 km Altitude | Revisit Time (Minutes) 1300 km Altitude |
|-------------------|----------------|----------------|-----------------------------|--|--|--|---|
| 1 | 1 | 1 | 0 | 678.5 | 361.0 | 313.8 | 301.1 |
| 1 | 1 | 1 | 30 | 566.4 | 301.8 | 259.2 | 244.1 |
| 1 | 1 | 1 | 60 | 300.7 | 118.2 | 117.1 | 127.3 |
| 1 | 1 | 1 | 90 | 95.9 | 102.6 | 111.2 | 123.0 |
| 2 | 2 | 2 | 0 | 339.3 | 180.5 | 156.9 | 150.6 |
| 2 | 2 | 2 | 30 | 283.2 | 150.9 | 129.6 | 122.1 |
| 2 | 2 | 2 | 60 | 150.4 | 59.1 | 58.6 | 63.7 |
| 2 | 2 | 2 | 90 | 48.0 | 51.3 | 55.6 | 61.5 |
| 3 | 4 | 4 | 0 | 169.6 | 90.3 | 78.5 | 75.3 |
| 3 | 4 | 4 | 30 | 141.6 | 75.5 | 64.8 | 61.0 |
| 3 | 4 | 4 | 60 | 75.2 | 29.6 | 29.3 | 31.8 |
| 3 | 4 | 4 | 90 | 24.0 | 25.7 | 27.8 | 30.8 |
| 4 | 6 | 6 | 0 | 113.1 | 60.2 | 52.3 | 50.2 |
| 4 | 6 | 6 | 30 | 94.4 | 50.3 | 43.2 | 40.7 |
| 4 | 6 | 6 | 60 | 50.1 | 19.7 | 19.5 | 21.2 |
| 4 | 6 | 6 | 90 | 16.0 | 17.1 | 18.5 | 20.5 |
| 5 | 8 | 8 | 0 | 84.8 | 45.1 | 39.2 | 37.6 |
| 5 | 8 | 8 | 30 | 70.8 | 37.7 | 32.4 | 30.5 |
| 5 | 8 | 8 | 60 | 37.6 | 14.8 | 14.6 | 15.9 |
| 5 | 8 | 8 | 90 | 12.0 | 12.8 | 13.9 | 15.4 |

The bar plot in Figure 6 provides a comprehensive overview of the contact duration between a set of IoT nodes at various latitudes on Mars and a constellation of satellites in different orbital configurations. The contact duration is when a satellite remains in direct line-of-sight with an IoT node, facilitating uninterrupted communication. Each subplot corresponds to a different IoT node at 0-, 30-, 60-, and 90-degree latitudes, respectively. The satellites are categorized by altitude (100, 500, 900, and 1300 km) and inclination (0, 30, 60, and 90 degrees), with the bars color-coded to distinguish between the altitudes. Analysis of the plots indicates that higher-altitude satellites generally provide longer contact durations due to their broader line-of-sight horizons. The most extended average contact times are observed with the satellite at a 1300 km altitude and 90-degree inclination, highlighting the impact of higher vantage points and polar orbit paths on communication windows. Conversely, satellites at lower altitudes tend to have shorter contact durations due to their closer proximity and faster orbital velocity, resulting in quicker transits across the IoT node’s sky. Notably, the inclination of the satellites also plays a significant role, with those in equatorial orbits (0-degree inclination) demonstrating the shortest contact times, particularly for IoT nodes situated at the poles.

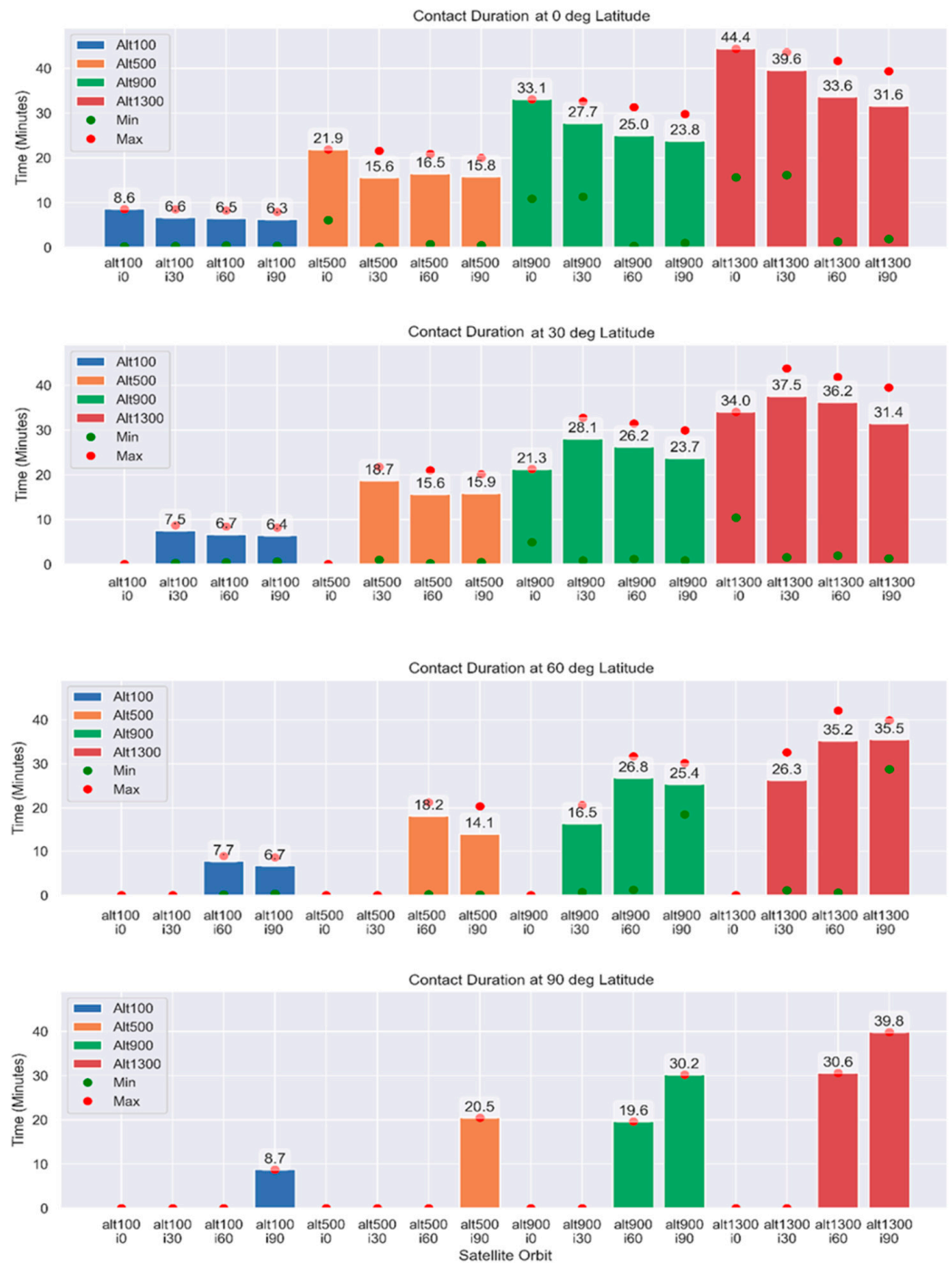


Figure 6. Contact duration for all analyzed Mars orbits and IoT devices at 0, 30, 60, and 90 degrees of latitude on Mars’s surface.

The bar plots in Figure 7 delineate the revisit time for IoT nodes stationed at varied latitudes on Mars, representing the interval required for satellites in the constellation to re-establish communication with given IoT nodes on the Martian surface. The analysis shows that the revisit time varies across satellite configurations, with higher altitudes typically manifesting reduced gaps due to the extensive coverage footprint. This is particularly noticeable for the 100 km altitude satellites, which exhibit the most extended gaps across all latitudes. Moreover, the plots reveal that the revisit time is not only a function of altitude but is also significantly influenced by orbital inclination. Notably, the minimum revisit time is often associated with lower inclination angles.

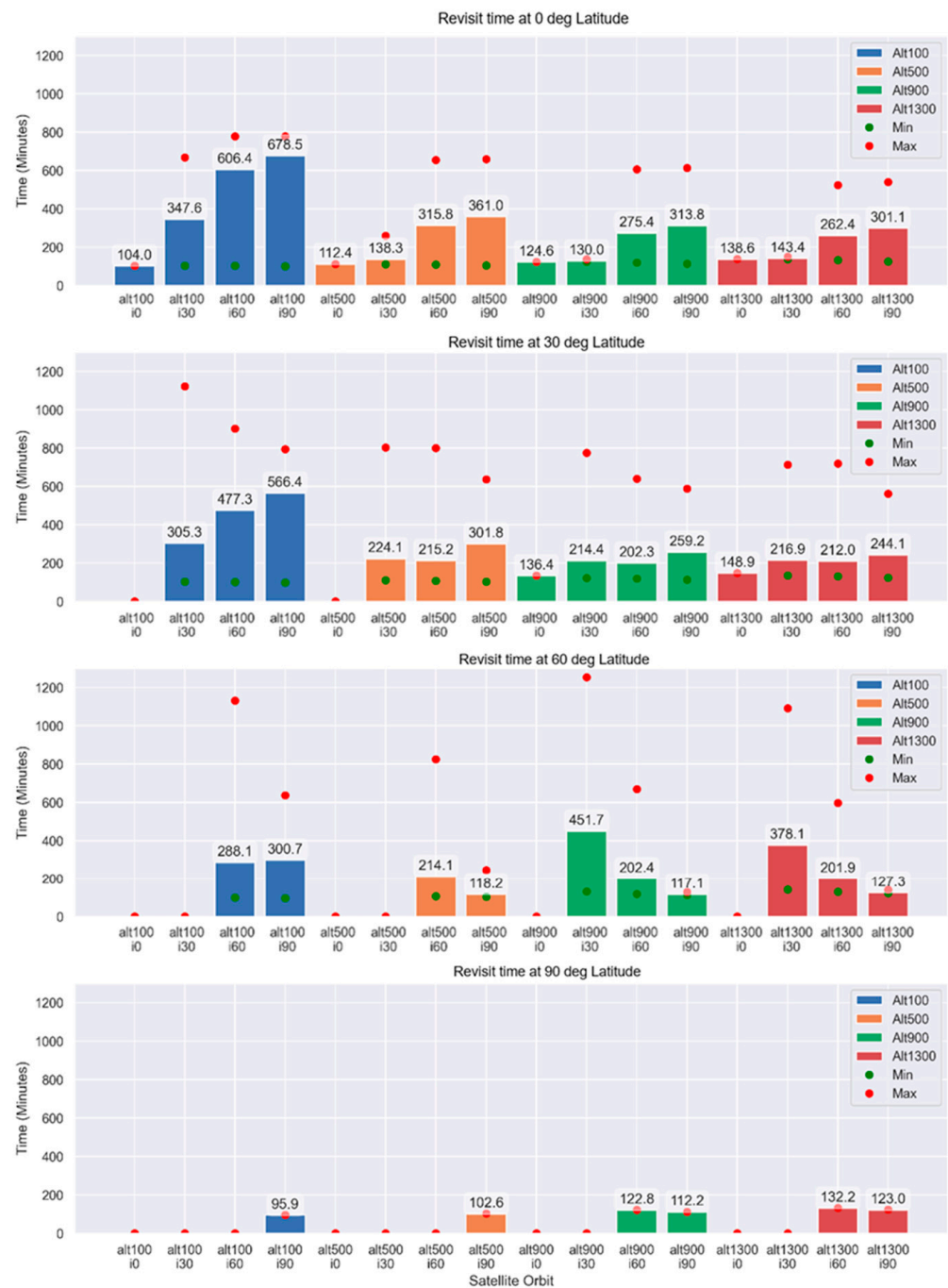


Figure 7. Revisit time for all analyzer Mars orbits and IoT devices at 0, 30, 60, and 90 degrees of latitude on Mars’s surface.

According to these findings, it is recommended to use inclination angles close to 90 degrees to ensure complete coverage due to their scientific significance. As for the satellites’ altitude, a higher altitude reduces the time it takes to revisit a location but also increases the communication distance between the IoT node and the satellite. On the other hand, a lower altitude reduces the contact duration and is more affected by the Doppler effect. An intermediate altitude of 500 km may be the most appropriate for both cases.

To increase the frequency of revisiting a specific location on Mars, the number of satellites in orbit can be increased. Table 3 provides details of the revisit times for various satellite constellation configurations around Mars, with an inclination of 90 degrees. These configurations differ based on the number of satellites, their orbital altitude, and the latitude

of the IoT node, as per the Walker Star model proposal. As the number of satellites in a constellation increases, the frequency at which the satellites revisit a specific location decreases significantly. Among the evaluated configurations, a constellation with six or more satellites orbiting at an altitude of 500 km or greater would provide visit times of less than an hour and 20.5 min at the equator and even less for polar areas. This configuration would be optimal for receiving data from IoT nodes on the surface. Constellations with six or more satellites and 500 km high orbits reduce revisit times considerably compared to configurations with fewer satellites.

The transmission distance simulation is performed using the Friis Model Transmission Equation in MATLAB. The simulation tests distances up to 2000 km between the IoT node and orbiting satellites, measuring the power received at the satellite. If the received power exceeds the receiver's sensitivity, the satellite can receive the transmission from the IoT node. Table 4 shows the parameters used in the simulation.

Table 4. Key simulation parameters.

| Parameters | Value | Parameters | Value |
|------------------------------|-------------|---------------------------|----------|
| Carrier frequency | 868/433 MHz | Antenna gains (reception) | 22.6 dBi |
| Transmit power | 14 dBm | Orbit height | 500 km |
| Receiver sensitivity | −137 dBm | Mars radius | 3390 km |
| Antenna gains (transmission) | 2.15 dBi | IoT node maximum distance | 1909 km |

The reception sensitivity of satellites is usually between −120 and −140 dBm. In our study, we opted for a sensitivity of −137 dBm, which was also used in reference [51]. For the IoT node on Mars, the transmission power is set to 14 dBm, with a transmitting antenna gain of 2.15 dBi and a receiving antenna gain of 22.6 dBi. We evaluated the LoRa bands at 433 MHz and 868 MHz using a single channel, part of the LoRa standard for terrestrial and satellite communications [52].

Based on the calculations above, it is recommended to use 500 km orbits to deploy a satellite constellation designed for IoT communication, following the model of modern orbiters [28]. These satellites would enable the retransmission of communications using an ISL in S-band, as shown in Figure 2. The maximum communication distance between an IoT node on the Martian surface and the satellite at its farthest point on the Martian horizon can be estimated from this orbit. Using trigonometric calculations based on the radius of Mars indicated in Table 4, the maximum LoRa communication distance between an IoT node and a satellite orbiting at 500 km is 1909 km.

Figure 8 illustrates the relationship between the maximum transmission power and the maximum distance to the frequencies of interest. For 868 MHz, the maximum reception power at a 500 km distance from the IoT node is estimated to be −109 dBm, while at 1909 km, it is −117 dBm. For 433 MHz, the estimated maximum received power is −106 dBm at a 500 km distance, while at 1909 km, it is −120 dBm. Therefore, in all cases of interest, the power received in the satellite is higher than the sensitivity of −137 dBm. These results suggest that communications using LoRa technologies under the proposed conditions are feasible.

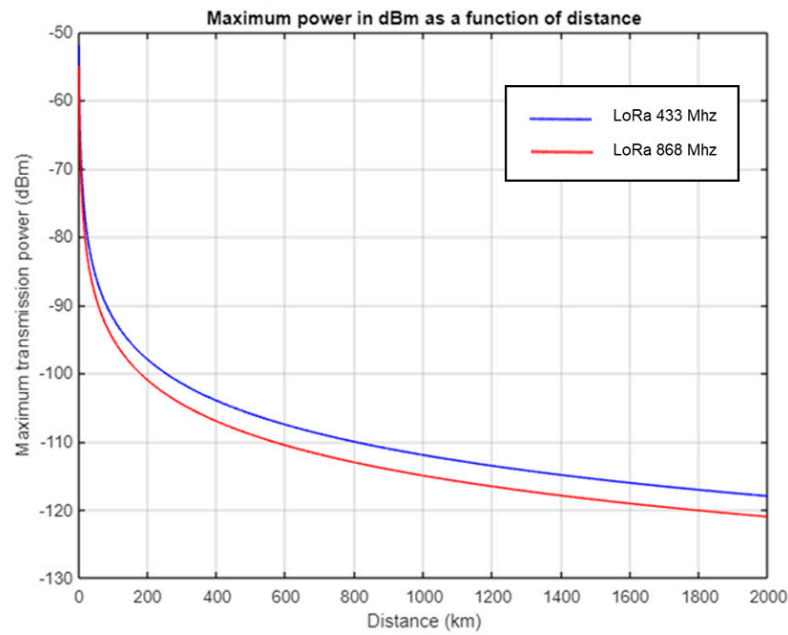


Figure 8. Maximum power related to distance using LoRa 433 MHz (in blue) and LoRa 868 MHz (in red).

The message capacity of LoRa satellites in the proposed architecture depends on the number of messages that can be received during each orbital period around Mars. This is determined by calculating the orbital period of the satellites using Kepler’s Third Law, resulting in a value of 122.7 min for a complete revolution around the planet. This calculation is essential to estimate the number of messages that can be processed by the satellite based on the data rate of each SF from theoretical IoT nodes.

Table 5 displays the capacity analysis using SF values for standard LoRa messages (message size of 25 bytes and a bandwidth of 125 kHz [53]). The packet values also include duration, which determines the time it takes for the message to be transmitted or received based on the SF and the message size.

Table 5. Spreading factor values for 25-byte messages at 125 KHz.

| SF | Data Rate (kbps) | Packet Duration (ms) |
|----|------------------|----------------------|
| 7 | 5.47 | 36 |
| 8 | 3.13 | 64 |
| 9 | 1.76 | 113 |
| 10 | 0.98 | 204 |
| 11 | 0.54 | 365 |
| 12 | 0.29 | 682 |

Figure 9 shows the theoretical maximum number of messages per SF for a satellite in Mars orbit. However, this is only an estimate as it does not consider interference, collisions, the actual hardware capacity of the satellite, or other factors that could affect message reception. Although an SF7 allows for more messages, SF12 is typically used for satellite communications as it is more robust and increases the probability of reception in orbiting satellites [54]. Therefore, the maximum theoretical number of messages a satellite could receive is 10,794 from IoT nodes per orbital period. This is much lower than other studies for IoT constellations in LEOs, which can handle up to 60,000 messages from IoT nodes per hour [55].

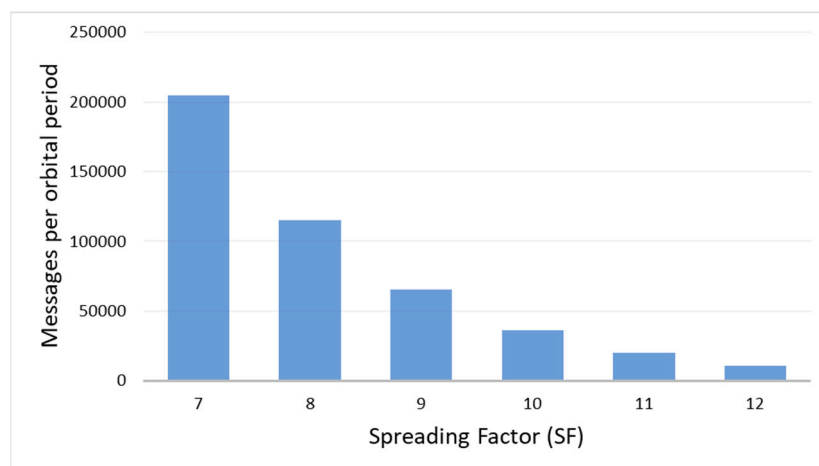


Figure 9. Message capacity per SF during the orbital period of a satellite on Mars.

A critical analysis component was the computation of visibility access using STK's advanced models for Light Time Delay and Apparent Position. The Light Time Delay model is essential for accounting for the duration required for light, or in this context, a signal, to traverse the distance from Earth to Mars, which is pivotal for grasping communication delays. The Apparent Position model calculates the perceived location of Mars orbiters from Earth, factoring in the finite speed of light and the orbital motion of both planets [56].

The data were exported to CSV files following the establishment of the required orbital propagations and communication links in STK. After this, the data underwent post-processing to facilitate the analysis of several metrics critical to comprehending the Earth–Mars communication link. These metrics include the following:

- Range: The distance (million kilometers) throughout the period.
- One-Way-Light Time (OWLT): The time it takes for a signal to propagate at the Earth–Mars range.
- Averaged Daily Contact Frequency: The average number of contacts every 24 h.
- Averaged Daily Contact Time: The aggregated contact time per day.

These metrics are vital for assessing the viability and reliability of communications between Earth's DSN and the Mars orbiters and are discussed below. The code for creating the STK scenario, exporting the data, and processing and plotting the results can be seen in the repository of the Data Availability Statement.

The characterization of the Earth-to-Mars link dynamics is essential for successful interplanetary communications. The analysis presented in this section explores the complex relationship between the range, communication time, and frequency of contacts as orbital mechanics and the positioning of ground stations on Earth influence them. Insights into the optimal conditions for establishing a stable communication link with Mars orbiters are provided, considering the inherent challenges presented by the relative movements of Earth and Mars and the limitations imposed by the planets' horizons.

Figure 10 (top) illustrates the dynamic nature of the Earth-to-Mars link, depicting the variation in range and OWLT between NASA's DSN ground sites and Mars. The data indicate a periodic oscillation ranging from 96 to 362 million kilometers, occurring over two years, which aligns with Earth and Mars's relative positions in their orbits. Correspondingly, OWLT varies between 5.3 and 20.1 min. These values indicate Earth's closest approach to Mars, known as opposition, and when they are on opposite sides of the Sun, known as conjunction. This cyclic pattern directly results from the orbital mechanics of the two planets and defines the planning backhauling strategies for Mars missions (see Figure 11).

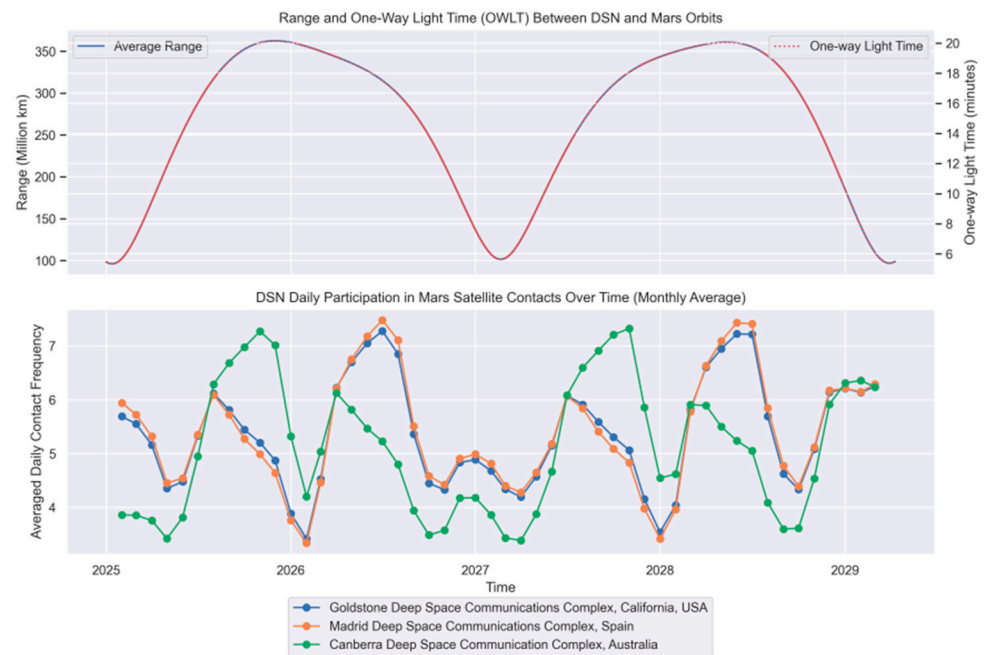


Figure 10. Range, OWLT (top), and participation of NASA’s DSN ground sites (bottom) in the contacts between Earth and Mars segments.

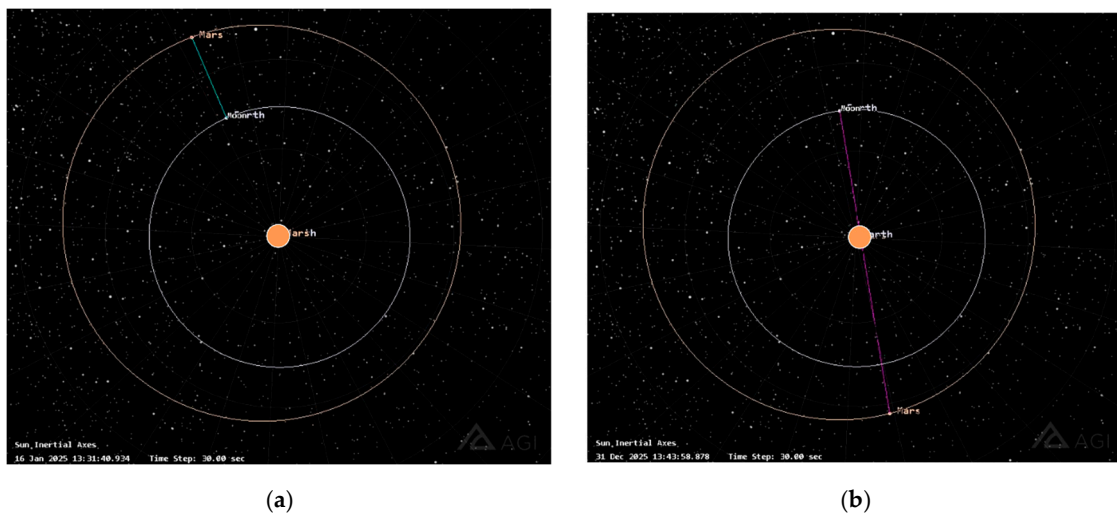


Figure 11. Far (a) and close (b) ranges between Earth and Mars.

Figure 10 (bottom) depicts the varying involvement of each DSN ground site in maintaining communication with Mars-orbiting spacecraft. The graph highlights a notable trend: The Canberra station in Australia consistently provides the highest communication frequency, particularly when Mars is optimally positioned for the southern hemisphere. Conversely, the Goldstone and Madrid stations exhibit increased contact when Mars is better aligned with the northern hemisphere. This pattern underscores the need for strategic planning in ground station resource allocation to accommodate the periodic nature of Earth–Mars connectivity for optimal mission support.

Figure 12 provides a detailed temporal analysis of daily contact frequency and duration between Earth’s DSN and Mars orbiters, segmented by altitude and inclination. Note that the aggregated daily contact time in Figure 12 considers the cumulative communication windows from all three DSN sites, so the total can exceed 24 h in a single day (see snapshot in Figure 13a).

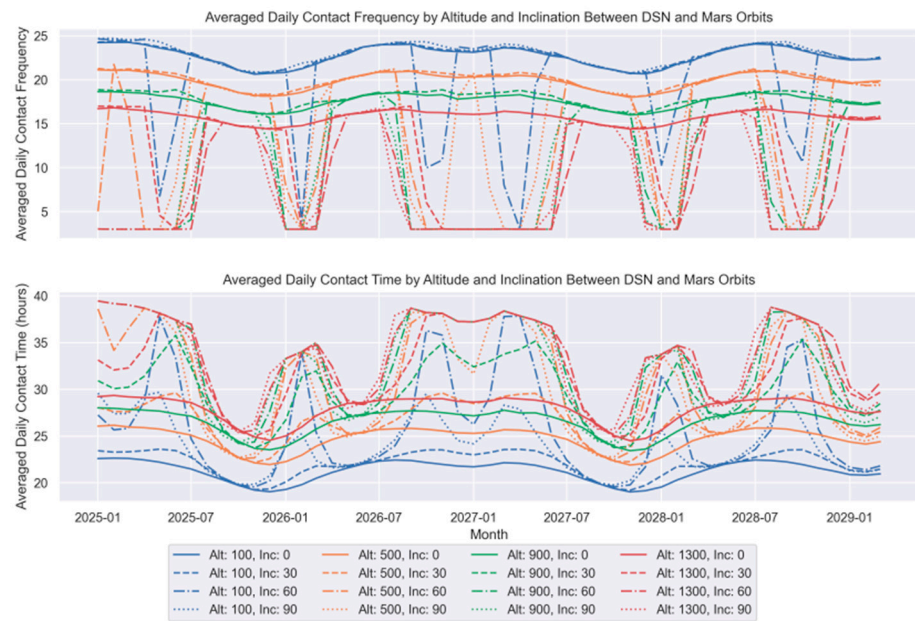


Figure 12. Time plots for daily contact frequency (top) and daily contact duration (bottom) for the 16 Mars orbits.

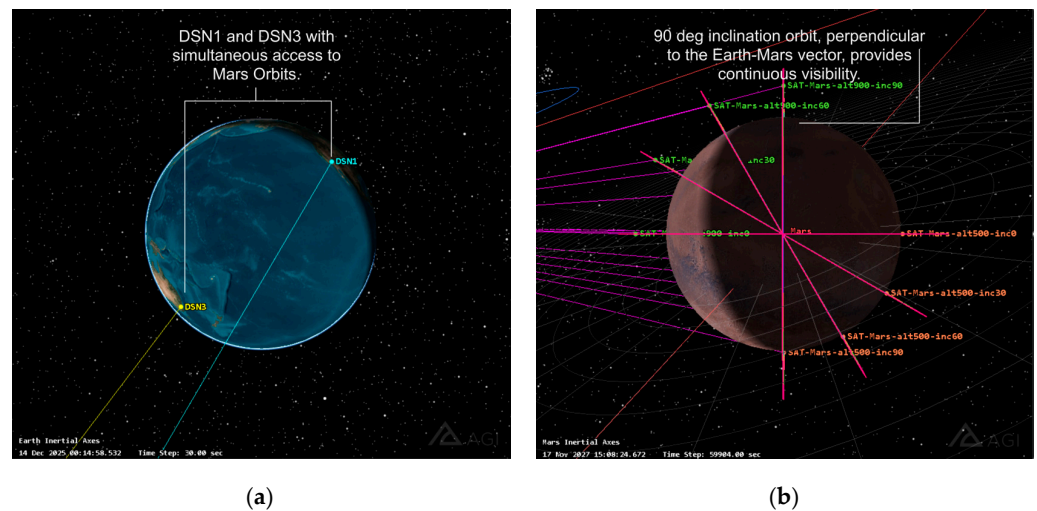


Figure 13. Scenario snapshots with two simultaneous DSNs in sight in (a) and 90-degree inclination orbit with permanent sight in (b).

The top plot in Figure 12 indicates that orbiters in low-altitude trajectories (100 km) exhibit the highest contact frequency, with 20 to 24 contacts per day, suggesting more frequent communication interruptions. These orbits also show the shortest aggregated contact durations, ranging from 20 to 27 h daily.

Medium- and high-altitude orbits (500 to 1300 km) demonstrate better performance, with daily contact times stretching from 24 to 40 h and fewer contact interruptions, between 14 and 16 per day. The polar orbits are marked by significant spikes, reflecting lengthy contact durations due to their alignment. This prevents the satellite from being occluded by Mars, thereby ensuring prolonged communication windows (see snapshot in Figure 13b).

Figure 14 shows the trade-off between daily contact frequency and duration for the 16 Mars orbiter scenarios. It effectively illustrates the inverse relationship between altitude and communication disruption: lower-altitude orbits experience increased frequency of contact but suffer from shorter durations due to the relative motion of Mars and Earth, causing more frequent occultations.

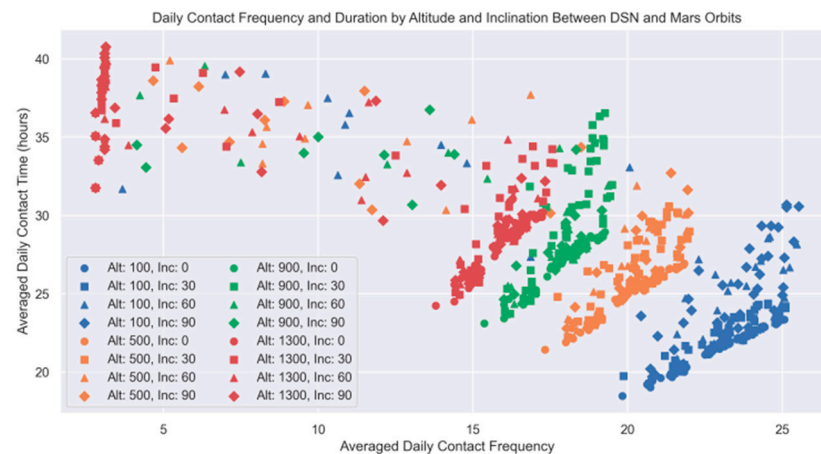


Figure 14. Scatter plot correlating the daily contact frequency and duration for each of the 16 Mars orbits.

Conversely, higher altitude orbits benefit from longer, more stable communication windows. This is attributed to their wider field of view above the Martian horizon, which remains unobstructed for extended periods even as Mars rotates.

The plot emphasizes the superior duration of contacts for higher altitudes, implying that satellites closer to Mars, despite being in a favorable orbital plane, still succumb to the planet's horizon, interrupting the line of sight necessary for continuous communication.

5. Potential IoT Applications on Mars

IoT technology can collect, analyze, and transmit data to optimize astronaut safety and study the Martian environment while facilitating remote monitoring from Earth. Some of the applications that would benefit from the inclusion of this technology are the following:

- **Agriculture:** A vital aspect of colonizing Mars and establishing human bases is the ability to produce food. Growing food in greenhouses is one of the most feasible methods for achieving sustainability and autonomy in future space missions [57]. Cultivating crops in Martian greenhouses can be conducted effectively with the help of sensors connected to IoT nodes. These sensors can monitor various parameters such as soil humidity, temperature, fertilizer concentration, soil hydrogen potential (pH) level, and more, allowing for optimization and efficient management of the crops.
- **Astrobiology and exobiology:** Exploring the possibility of extraterrestrial life on Mars is a priority objective in Martian exploration [58]. To aid in this search, IoT nodes can be deployed with sensors specifically designed to detect signs of life on Mars. These sensors may include temperature, humidity, pH, and organic compounds [59].
- **Meteorology:** IoT nodes can measure atmospheric parameters like temperature, pressure, and suspended particles. On Mars, weather data can be collected through stations such as the Environmental Rover Monitoring Station (REMS) or the Mars Environmental Dynamics Analyzer (MEDA) on rovers like Curiosity and Perseverance. This would help gather meteorological information from different areas of the planet and improve the detection of adverse weather conditions, like dust storms, which can cause harm to electronic systems [22], human habitats, and missions.
- **Surface exploration:** It involves using IoT nodes distributed across various areas of the planet. These nodes are equipped with specialized sensors, such as humidity and isotopic sensors, intended to identify water resources in the form of water or ice. They are also used to study the composition of the soil, particularly the regolith, for applications in construction [60] and agriculture [61]. Additionally, accelerometers are integrated into these IoT nodes to detect and analyze "marsquakes". Space radiation sensors are crucial for evaluating housing viability and defining safety protocols in future human-crewed missions [62]. Furthermore, IoT nodes with gas sensors are

suggested for detecting underground volatile compounds, such as methane, which could be helpful as a fuel source for spacecraft [63].

- Location systems: IoT-based location systems can help track and guide human explorers, as well as locate astronauts, equipment, or materials. These devices can be attached to astronauts or equipment and located using radio triangulation techniques [64], with connectivity protocols like LoRa [65], Bluetooth Low Energy (BLE), or Wi-Fi [66].
- Aerospace medicine: This refers to integrating sensors into astronauts' clothing, monitoring their vital signs during missions to Mars [67]. These sensors are connected to IoT nodes and can measure essential parameters such as heart rate, blood pressure, and oxygen level. By monitoring the health of astronauts remotely, this technology can help ensure their well-being during the missions.

6. Open Research Challenges

Potential future directions can be identified to continue advancing the use of IoT in Martian exploration. These encompass technological advancements, standardization efforts, and testing methodologies to ensure the robustness and scalability of the proposed architecture. The following specific areas at the crossroads of interplanetary networking and direct-to-satellite IoT could be explored in future research:

- Integration, interoperability, and standardization of delay tolerant networking (DTN) and LoRa/LoRaWAN: This integration presents an opportunity to enhance the resilience of interplanetary communication. The development of standardized protocols and interoperable systems is proposed to facilitate data transmission under varying networks and environmental conditions.
- Energy management techniques for the Martian environment: Given the unique environmental conditions on Mars, specialized energy management techniques for IoT devices are required. These could include advanced energy storage solutions and adaptive energy management algorithms to optimize the performance of IoT nodes on the Martian surface.
- Scalability and reliability testing: As the scope of IoT deployments on Mars expands, validating the robustness and effectiveness of the communication infrastructure becomes essential. Rigorous testing methodologies are needed to evaluate the system's ability to maintain reliable connectivity and scale to meet the changing demands of the Martian environment.
- Advanced interplanetary communication systems: The investigation of more advanced communication systems to handle the unique challenges of long-distance communication between Mars and Earth is proposed. This would include exploring new communication protocols, signal processing techniques, and data transmission methods to enhance the efficiency and reliability of interplanetary communication.
- Enhanced IoT applications on Mars: Expanding the scope of IoT applications on Mars is suggested by developing new sensor technologies, data collection methods, and analytical tools to support a wide range of scientific, environmental, and exploration applications on the Martian surface.
- Integration of artificial intelligence and machine learning: Integrating artificial intelligence and machine learning algorithms into the IoT framework for Martian exploration is proposed. This could enable autonomous decision-making, predictive analytics, and adaptive control systems to enhance the capabilities of Martian IoT devices and satellite constellations.
- Martian atmosphere and high-frequency communication: This involved the investigation of atmospheric effects and phenomena, like dust storms, on high-frequency communication to improve the performance of satellite communication with devices on the Martian surface.

7. Conclusions

The study has corroborated that the architecture designed for Martian exploration through IoT, using satellite constellations that use LoRa communications, is technically feasible and efficient. This is shown in various aspects, such as the range of communication, the transmission speed, the ability to handle the interactions of multiple IoT nodes, and the capacity of satellites to process messages. This determines the permissible density of IoT nodes. The study confirmed that the interaction between the nodes and the orbital satellites is viable, ensuring stable and reliable connectivity. The maximum effective communication distance between the IoT nodes on the surface of Mars and the satellites in orbit has been determined, and the communication periodicity has been based on the satellite revisit cycle. The feasibility of interplanetary communications between Mars and Earth has also been investigated, highlighting the need to understand the dynamics of communication links to ensure the efficiency and reliability of the system. The study also demonstrated the feasibility of implementing an extensive network of IoT nodes on Mars, given that the satellites can process a significant volume of messages during each orbit. Adopting this architecture predicts a substantial advance in the accumulation of Martian data, transcending the current restrictions of space missions and optimizing the interplanetary transmission of information collected by IoT devices that operate under LoRa technology. Finally, there are several areas where future research could be focused. These include the integration, interoperability, and standardization of DTN and LoRa/LoRaWAN; the development of energy management techniques that are suited to the Martian environment; testing for scalability and reliability; the design of advanced interplanetary communication systems; and the atmospheric effects on high-frequency communication. Additionally, there is potential for integrating artificial intelligence and machine learning technologies to improve the efficiency and safety of IoT deployments on Mars.

Author Contributions: Conceptualization and methodology, O.L., J.A.F. and P.L.; software and validation, O.L. and J.A.F.; writing—review and editing, O.L., J.A.F., P.L. and M.R.; visualization, M.A.S.; supervision, P.L. All authors have read and agreed to the published version of the manuscript.

Funding: This research was funded by Universidad Internacional de La Rioja, grant number JT-2022-04 (Project: “Arquitectura y sistema de comunicaciones para la conectividad con nanosatélites de baja órbita”). Also, it was funded by the Spanish Ministry of Science, Innovation and Universities under Project MIG-20231006 (“Diseño de chips innovadores para la primera placa integrada multifuncional de alto rendimiento y bajo consumo energético en globos estratosféricos”). Part of this work was supported by EU’s H2020 R&D program under the Marie Skłodowska-Curie grant agreement No 101008233 (MISSION project) and the French National Research Agency (ANR) project ANR-22-CE25-0014-01.

Data Availability Statement: All the materials developed in this work with STK are freely available in the repository: <https://gitlab.inria.fr/jfnaire/earth-mars-link-characterization> (accessed on 17 February 2024).

Conflicts of Interest: The authors declare no conflicts of interest.

References

1. Kua, J.; Loke, S.W.; Arora, C.; Fernando, N.; Ranaweera, C. Internet of Things in Space: A Review of Opportunities and Challenges from Satellite-Aided Computing to Digitally-Enhanced Space Living. *Sensors* **2021**, *21*, 8117. [[CrossRef](#)] [[PubMed](#)]
2. Kerrouche, K.D.E.; Wang, L.; Seddjar, A.; Rastinasab, V.; Oukil, S.; Ghaffour, Y.M.; Nouar, L. Applications of Nanosatellites in Constellation: Overview and Feasibility Study for a Space Mission Based on Internet of Space Things Applications Used for AIS and Fire Detection. *Sensors* **2023**, *23*, 6232. [[CrossRef](#)] [[PubMed](#)]
3. Akyildiz, I.F.; Kak, A. The Internet of Space Things/CubeSats. *IEEE Netw.* **2019**, *33*, 212–218. [[CrossRef](#)]
4. Hassan, S.S.; Park, Y.M.; Tun, Y.K.; Saad, W.; Han, Z.; Hong, C.S. SpaceRIS: LEO Satellite Coverage Maximization in 6G Sub-THz Networks by MAPPO DRL and Whale Optimization. *IEEE J. Sel. Areas Commun.* **2024**. [[CrossRef](#)]
5. Allen, P.; Wickham-Eade, J.; Trichas, M. The Potential of Small Satellites for Scientific and Astronomical Discovery. *Nat. Astron.* **2020**, *4*, 1039–1042. [[CrossRef](#)]

6. Rometsch, F.A.A.S.D.T.; Casini, A.E.M.; Drepper, A.; Cowley, A.; de Winter, J.C.F.; Guo, J. Design and Evaluation of an Augmented Reality Tool for Future Human Space Exploration Aided by an Internet of Things Architecture. *Adv. Space Res.* **2022**, *70*, 2145–2166. [[CrossRef](#)]
7. Nazari-Sharabian, M.; Aghababaei, M.; Karakouzian, M.; Karami, M. Water on Mars—A Literature Review. *Galaxies* **2020**, *8*, 40. [[CrossRef](#)]
8. Bell, J.F.; Maki, J.N.; Mehall, G.L.; Ravine, M.A.; Caplinger, M.A.; Bailey, Z.J.; Brylow, S.; Schaffner, J.A.; Kinch, K.M.; Madsen, M.B.; et al. The Mars 2020 Perseverance Rover Mast Camera Zoom (Mastcam-Z) Multispectral, Stereoscopic Imaging Investigation. *Space Sci. Rev.* **2021**, *217*, 24. [[CrossRef](#)] [[PubMed](#)]
9. Giacomini, E.; Westerberg, L.-G.; Nikolakopoulos, G. A Survey on Drones for Planetary Exploration: Evolution and Challenges. In Proceedings of the 2022 30th Mediterranean Conference on Control and Automation (MED), Athens, Greece, 28 June–1 July 2022; pp. 583–590.
10. Levchenko, I.; Xu, S.; Wu, Y.-L.; Bazaka, K. Hopes and Concerns for Astronomy of Satellite Constellations. *Nat. Astron.* **2020**, *4*, 1012–1014. [[CrossRef](#)]
11. Arzo, S.T.; Sikeridis, D.; Devetsikiotis, M.; Granelli, F.; Fierro, R.; Esmaeili, M.; Akhavan, Z. Essential Technologies and Concepts for Massive Space Exploration: Challenges and Opportunities. *IEEE Trans. Aerosp. Electron. Syst.* **2023**, *59*, 3–29. [[CrossRef](#)]
12. Liu, T.; Jiang, H.; Yang, Z.; Chen, Z. Reconfigurable Intelligent Surface Enhanced Massive IoT Systems with Nonlinear Measurements. *IEEE Wirel. Commun. Lett.* **2023**, *12*, 1976–1980. [[CrossRef](#)]
13. Jiang, H.; Mukherjee, M.; Zhou, J.; Lloret, J. Channel Modeling and Characteristics for 6G Wireless Communications. *IEEE Netw.* **2021**, *35*, 296–303. [[CrossRef](#)]
14. Ledesma, O.; Lamo, P.; Fraire, J.A. Trends in LPWAN Technologies for LEO Satellite Constellations in the NewSpace Context. *Electronics* **2024**, *13*, 579. [[CrossRef](#)]
15. Marcozzi, M.; Ottavi, M. Evaluation of a Multi-Access Communication Architecture for Future Mars Exploration. In Proceedings of the 38th International Communications Satellite Systems Conference (ICSSC 2021), Arlington, VA, USA, 27–30 September 2021. [[CrossRef](#)]
16. Molli, S.; Durante, D.; Boscagli, G.; Cascioli, G.; Racioppa, P.; Alessi, E.M.; Simonetti, S.; Vigna, L.; Iess, L. Design and Performance of a Martian Autonomous Navigation System Based on a Smallsat Constellation. *Acta Astronaut.* **2023**, *203*, 112–124. [[CrossRef](#)]
17. Fraire, J.A.; Iova, O.; Valois, F. Space-Terrestrial Integrated Internet of Things: Challenges and Opportunities. *IEEE Commun. Mag.* **2022**, *60*, 64–70. [[CrossRef](#)]
18. Wan, P.; Zhan, Y.; Pan, X.; Huang, L. Scheduling Algorithm for the Multiple Rovers' Access to Single Orbiter on the Mars Relay Communication Links. *Int. J. Satell. Commun. Netw.* **2019**, *37*, 612–629. [[CrossRef](#)]
19. Murthy, S.; Sareen, A.; John, E.O.; Jayaraman, P.; S, M.H. Orbital Exploration of Phobos by a Nano-Satellite Using Solar Electric Propulsion. In Proceedings of the 2022 IEEE Aerospace Conference (AERO), Big Sky, MT, USA, 5–12 March 2022; pp. 1–11.
20. Zeedan, A.; Khattab, T. CubeSat Communication Subsystems: A Review of On-Board Transceiver Architectures, Protocols, and Performance. *IEEE Access* **2023**, *11*, 88161–88183. [[CrossRef](#)]
21. Restier-Verlet, J.; el Nachef, L.; Ferlazzo, M.; Choboq, J.; Granzotto, A.; Bouchet, A.; Foray, N. Radiation on Earth or in Space: What Does It Change? *Int. J. Mol. Sci.* **2021**, *22*, 3739. [[CrossRef](#)] [[PubMed](#)]
22. Karpovich, E.; Kombaev, T.; Gueraiche, D.; Evdokimova, D.; Alexandrov, K. Long-Endurance Mars Exploration Flying Vehicle: A Project Brief. *Aerospace* **2023**, *10*, 965. [[CrossRef](#)]
23. Mahattanavuttakorn, S.; Tiputhai, K.; Senivong, P.; Putsa, N.; Namkotr, W.; Tancharoensup, C.; Chancharoen, W. A Comprehensive Review of Thermal Control of Moveable and Non-Moveable Spacecraft in Mars Sample Collecting Mission. *Eng. J.* **2023**, *27*, 85–98. [[CrossRef](#)]
24. Mortazavi, S.; Mortazavi, S.A.; Sihver, L. Can Adaptive Response and Evolution Make Survival of Extremophile Bacteria Possible on Mars? In Proceedings of the 2020 IEEE Aerospace Conference, Big Sky, MT, USA, 7–14 March 2020; pp. 1–6.
25. Zaman, F.A.; Townsend, L.W.; Burahmah, N.T. Radiation Risks in a Mission to Mars for a Solar Particle Event Similar to the AD 993/4 Event. *Aerospace* **2021**, *8*, 143. [[CrossRef](#)]
26. Janssen, T.; Koppert, A.; Berkvens, R.; Weyn, M. A Survey on IoT Positioning Leveraging LPWAN, GNSS, and LEO-PNT. *IEEE Internet Things J.* **2023**, *10*, 11135–11159. [[CrossRef](#)]
27. Chen, Q.; Yang, L.; Liu, X.; Guo, J.; Wu, S.; Chen, X. Multiple Gateway Placement in Large-Scale Constellation Networks with Inter-Satellite Links. *Int. J. Satell. Commun. Netw.* **2021**, *39*, 47–64. [[CrossRef](#)]
28. Moeller, G.; Ao, C.O.; Mannucci, A.J. Tomographic Radio Occultation Methods Applied to a Dense Cubesat Formation in Low Mars Orbit. *Radio Sci.* **2021**, *56*, e07199. [[CrossRef](#)]
29. Campbell, B.A.; Morgan, G.A.; Bernardini, F.; Putzig, N.E.; Nunes, D.C.; Plaut, J.J. Calibration of Mars Reconnaissance Orbiter Shallow Radar (SHARAD) Data for Subsurface Probing and Surface Reflectivity Studies. *Icarus* **2021**, *360*, 114358. [[CrossRef](#)]
30. Koktas, E.; Basar, E. Communications for the Planet Mars: Past, Present, and Future. *arXiv* **2022**, arXiv:2211.14245. [[CrossRef](#)]
31. Nagle-McNaughton, T.P.; Scuderi, L.A.; Erickson, N. Squeezing Data from a Rock: Machine Learning for Martian Science. *Geosciences* **2022**, *12*, 248. [[CrossRef](#)]
32. Budroweit, J.; Patscheider, H. Risk Assessment for the Use of COTS Devices in Space Systems under Consideration of Radiation Effects. *Electronics* **2021**, *10*, 1008. [[CrossRef](#)]

33. Gutiérrez, O.; Prieto, M.; Perales-Eceiza, A.; Ravanbakhsh, A.; Basile, M.; Guzmán, D. Toward the Use of Electronic Commercial Off-the-Shelf Devices in Space: Assessment of the True Radiation Environment in Low Earth Orbit (LEO). *Electronics* **2023**, *12*, 4058. [CrossRef]
34. Kimura, S.; Sawada, H.; Saiki, T.; Mimasu, Y.; Ogawa, K.; Tsuda, Y. Deep Space In Situ Imaging Results of Commercial Off-the-Shelf Visual Monitoring System Aboard the Hayabusa2 Spacecraft. *IEEE Aerosp. Electron. Syst. Mag.* **2021**, *36*, 16–23. [CrossRef]
35. Capez, G.M.; Henn, S.; Fraire, J.A.; Garelo, R. Sparse Satellite Constellation Design for Global and Regional Direct-to-Satellite IoT Services. *IEEE Trans. Aerosp. Electron. Syst.* **2022**, *58*, 3786–3801. [CrossRef]
36. Balaram, J.; Aung, M.; Golombek, M.P. The Ingenuity Helicopter on the Perseverance Rover. *Space Sci. Rev.* **2021**, *217*, 56. [CrossRef]
37. Ghazali, M.H.M.; Teoh, K.; Rahiman, W. A Systematic Review of Real-Time Deployments of UAV-Based LoRa Communication Network. *IEEE Access* **2021**, *9*, 124817–124830. [CrossRef]
38. Zhou, Z.; Afhamisis, M.; Palattella, M.R.; Accettura, N.; Berthou, P. Pervasive LPWAN Connectivity through LEO Satellites: Trading off Reliability, Throughput, Latency, and Energy Efficiency. In *Low-Power Wide-Area Networks: Opportunities, Challenges, Risks and Threats*; Springer: Cham, Switzerland, 2022. [CrossRef]
39. Leenders, G.; Callebaut, G.; Ottoy, G.; Van der Perre, L.; De Strycker, L. Multi-RAT for IoT: The Potential in Combining LoRaWAN and NB-IoT. *IEEE Commun. Mag.* **2021**, *59*, 98–104. [CrossRef]
40. Marini, R.; Mikhaylov, K.; Pasolini, G.; Buratti, C. Low-Power Wide-Area Networks: Comparison of LoRaWAN and NB-IoT Performance. *IEEE Internet Things J.* **2022**, *9*, 21051–21063. [CrossRef]
41. Chan, C.C.; Al Homssi, B.; Al-Hourani, A. Performance Evaluation of Random Access Methods for IoT-over-Satellite. *Remote Sens.* **2022**, *14*, 4232. [CrossRef]
42. Fraire, J.A.; Céspedes, S.; Accettura, N. Direct-To-Satellite IoT-A Survey of the State of the Art and Future Research Perspectives. In *Proceedings of the Ad-Hoc, Mobile, and Wireless Networks*; Palattella, M.R., Scanzio, S., Coleri Ergen, S., Eds.; Springer International Publishing: Cham, Switzerland, 2019; pp. 241–258.
43. Leyva-Mayorga, I.; Soret, B.; Röper, M.; Wübben, D.; Matthiesen, B.; Dekorsy, A.; Popovski, P. LEO Small-Satellite Constellations for 5G and Beyond-5G Communications. *IEEE Access* **2020**, *8*, 184955–184964. [CrossRef]
44. Zhang, Y.; Bai, S.; Han, C. Geometric Analysis of a Constellation with a Ground Target. *Acta Astronaut.* **2022**, *191*, 510–521. [CrossRef]
45. Jung, S.; Im, G.; Jung, D.-H.; Kim, P.; Ryu, J.G.; Kang, J. Performance Analysis of DSSS- and CSS-Based Physical Layer for IoT Transmission over LEO Satellites. *ETRI J.* **2022**, *44*, 543–559. [CrossRef]
46. Dezfouli, A.; Rahbari Manesh, K.; Kheirikhah, M.M.; Soheili, J. A Review of Physical and Environmental Components of Habitat Design on Mars. *Creat. City Des.* **2023**, *6*, 59–77.
47. Xiu-min, H.; Jiang-hui, J. The Recent Research Progress of Exoplanets of Ultra-Short Periods. *Chin. Astron. Astrophys.* **2020**, *44*, 283–312. [CrossRef]
48. Rahman, H.U.; Ahmad, M.; Ahmad, H.; Habib, M.A. LoRaWAN: State of the Art, Challenges, Protocols and Research Issues. In *Proceedings of the 2020 IEEE 23rd International Multitopic Conference (INMIC)*, Bahawalpur, Pakistan, 5–7 November 2020; pp. 1–6.
49. Aggarwal, S.; Nasipuri, A. Improving Scalability of LoRaWAN Networks by Spreading Factor Distribution. In *Proceedings of the SoutheastCon 2021*, Atlanta, GA, USA, 10–13 March 2021; pp. 1–7.
50. Höyhty, M.; Boumard, S.; Yastrebova, A.; Järvensivu, P.; Kiviranta, M.; Anttonen, A. Sustainable Satellite Communications in the 6G Era: A European View for Multilayer Systems and Space Safety. *IEEE Access* **2022**, *10*, 99973–100005. [CrossRef]
51. Ullah, M.A.; Mikhaylov, K.; Alves, H. Analysis and Simulation of LoRaWAN LR-FHSS for Direct-to-Satellite Scenario. *IEEE Wirel. Commun. Lett.* **2022**, *11*, 548–552. [CrossRef]
52. Kiki, M.J.M.; Iddi, I. Improved LORA Modulation Output in LEO Satellite Internet of Things. *J. Electr. Eng. Technol.* **2022**, *17*, 1379–1387. [CrossRef]
53. Lim, J.-T.; Han, Y. Spreading Factor Allocation for Massive Connectivity in LoRa Systems. *IEEE Commun. Lett.* **2018**, *22*, 800–803. [CrossRef]
54. Álvarez, G.; Fraire, J.A.; Hassan, K.A.; Céspedes, S.; Pesch, D. Uplink Transmission Policies for LoRa-Based Direct-to-Satellite IoT. *IEEE Access* **2022**, *10*, 72687–72701. [CrossRef]
55. Maleki, A.; Nguyen, H.H.; Barton, R. Outage Probability Analysis of LR-FHSS in Satellite IoT Networks. *IEEE Commun. Lett.* **2023**, *27*, 946–950. [CrossRef]
56. Ansys Government Initiatives (AGI). Light Time Delay and Apparent Position. Available online: <https://help.agi.com/stk/LinkedDocuments/LightTimeDelayandApparentPosition.pdf> (accessed on 27 February 2024).
57. Oze, C.; Beisel, J.; Dabsys, E.; Dall, J.; North, G.; Scott, A.; Lopez, A.M.; Holmes, R.; Fendorf, S. Perchlorate and Agriculture on Mars. *Soil Syst.* **2021**, *5*, 37. [CrossRef]
58. Enya, K.; Yamagishi, A.; Kobayashi, K.; Yoshimura, Y. Comparative Study of Methods for Detecting Extraterrestrial Life in Exploration Mission of Mars and the Solar System. *Life Sci. Space Res.* **2022**, *34*, 53–67. [CrossRef] [PubMed]

59. Baqué, M.; Backhaus, T.; Meeßen, J.; Hanke, F.; Böttger, U.; Ramkissoon, N.; Olsson-Francis, K.; Baumgärtner, M.; Billi, D.; Cassaro, A.; et al. Biosignature Stability in Space Enables Their Use for Life Detection on Mars. *Sci. Adv.* **2022**, *8*, eabn7412. [[CrossRef](#)] [[PubMed](#)]
60. Snehal, K.; Sinha, P.; Chaunsali, P. Development of Waterless Extra-Terrestrial Concrete Using Martian Regolith. *Adv. Space Res.* **2024**, *73*, 933–944. [[CrossRef](#)]
61. Kasiviswanathan, P.; Swanner, E.D.; Halverson, L.J.; Vijayapalani, P. Farming on Mars: Treatment of Basaltic Regolith Soil and Briny Water Simulants Sustains Plant Growth. *PLoS ONE* **2022**, *17*, e0272209. [[CrossRef](#)]
62. Montesinos, C.A.; Khalid, R.; Cristea, O.; Greenberger, J.S.; Epperly, M.W.; Lemon, J.A.; Boreham, D.R.; Popov, D.; Gorthi, G.; Ramkumar, N.; et al. Space Radiation Protection Countermeasures in Microgravity and Planetary Exploration. *Life* **2021**, *11*, 829. [[CrossRef](#)] [[PubMed](#)]
63. Kruyer, N.S.; Realf, M.J.; Sun, W.; Genzale, C.L.; Peralta-Yahya, P. Designing the Bioproduction of Martian Rocket Propellant via a Biotechnology-Enabled in Situ Resource Utilization Strategy. *Nat. Commun.* **2021**, *12*, 6166. [[CrossRef](#)] [[PubMed](#)]
64. Chen, B.; Ma, J.; Zhang, L.; Zhou, J.; Fan, J.; Lan, H. Research Progress of Wireless Positioning Methods Based on RSSI. *Electronics* **2024**, *13*, 360. [[CrossRef](#)]
65. Marquez, L.E.; Calle, M. Understanding LoRa-Based Localization: Foundations and Challenges. *IEEE Internet Things J.* **2023**, *10*, 11185–11198. [[CrossRef](#)]
66. Rathnayake, R.M.M.R.; Maduranga, M.W.P.; Tilwari, V.; Dissanayake, M.B. RSSI and Machine Learning-Based Indoor Localization Systems for Smart Cities. *Eng* **2023**, *4*, 1468–1494. [[CrossRef](#)]
67. Aravindhan, A.; Laxmikanth, G.; Shanmuga S., P.; Kamalraj, S. Medical Diagnosis during Space Tourism and Future Mars Colonization. In Proceedings of the 2020 6th International Conference on Advanced Computing and Communication Systems (ICACCS), Coimbatore, India, 6–7 March 2020; pp. 557–559.

Disclaimer/Publisher’s Note: The statements, opinions and data contained in all publications are solely those of the individual author(s) and contributor(s) and not of MDPI and/or the editor(s). MDPI and/or the editor(s) disclaim responsibility for any injury to people or property resulting from any ideas, methods, instructions or products referred to in the content.